

Higher-order stimulated Brillouin scattering with nondiffracting beams

I. Velchev and W. Ubachs

Laser Centre, Vrije Universiteit Amsterdam, De Boelelaan 1081, 1081-HV Amsterdam, The Netherlands

Received October 5, 2000

We report on an experimental investigation of stimulated Brillouin scattering pumped with a Bessel beam. Owing to the extended interaction length along the diffraction-free propagation, higher-order Stokes components are generated in a bulk Brillouin-active medium with odd and even orders propagating in opposite directions. The spatial, spectral, and temporal properties of the interacting waves are discussed. © 2001 Optical Society of America

OCIS codes: 290.5830, 190.4420, 190.5940.

Stimulated Brillouin scattering (SBS) first attracted the attention of the laser-physics community because of its phase-conjugation properties, an effect widely used for wave-front correction in powerful amplifier systems. In the 1970's SBS was studied in optical fibers, in which long interaction lengths can be achieved, significantly lowering the SBS threshold. Effects such as higher-order Stokes and anti-Stokes generation,¹ four-wave mixing, and self-phase modulation were investigated²; the concepts of a Brillouin fiber laser and Brillouin mode locking were also introduced.³ In the 1980's the first experimental observation of pulse compression by SBS was published,⁴ which triggered great interest with the prospect of achieving high peak intensities with nearly 100% conversion efficiency. During the two decades that followed, pulse energies of more than 1 J were compressed,⁵ subphoton-lifetime pulses were achieved,⁶ and compression ratios greater than 20 were realized by use of Gaussian beams.

In 1987 the concept of diffraction-free beams was introduced by Durnin and co-workers.^{7,8} They pointed out that the Helmholtz equation, apart from its trivial plane-wave solution, possesses a whole class of diffraction-free solutions, the simplest being a monochromatic wave propagating along the z axis with amplitude

$$\Phi(\rho, \theta, z; k) = \exp(i\beta z)J_0(\alpha\rho), \quad (1)$$

where $\rho^2 = x^2 + y^2$, $\alpha^2 + \beta^2 = k^2$, and J_0 is the zero-order Bessel function. This wave has a central maximum with half-width $\sim\alpha^{-1}$ surrounded by concentric ring-shaped maxima with amplitudes decaying as $\rho^{-1/2}$. The total energy of such a beam is infinite, since each lobe carries approximately the same energy as the preceding one.⁹ This fact makes it practically impossible to generate a nondiffracting beam for an infinite propagation distance.

If the Bessel beam is modulated by a Gaussian function $\exp(-\rho^2/w^2)$, the total energy in the beam is finite. This makes Bessel-Gauss beams¹⁰ experimentally feasible and limits the diffraction-free propagation to distances $L = w/\gamma$, where γ is the angular half-aperture of the cone of the Bessel beam [$\alpha = k \sin(\gamma)$]. A Bessel-Gauss beam with $w = 5$ mm and a cone angle of $2\gamma = 2.5^\circ$ is nearly nondiffracting

for a distance $L \approx 25$ cm, creating an intense line focus with a constant diameter of a few micrometers. The application of such a beam in nonlinear processes offers a number of unique possibilities.¹¹⁻¹⁷ Important advantages of Bessel pump beams over Gaussian ones are that (i) the scattering products in the far field can be spatially separated from the pump beam and (ii) the pump beam experiences no self-phase modulation, owing to the fact that it traverses the long line focus at an angle, resulting in high-peak-power interaction length of the order of the line-focus diameter (i.e., a few micrometers), whereas for the on-axis scattered beam the interaction length is $\sim L$. In the case of third-harmonic generation, the noncollinear phase matching within the conical beam showed the novel effect of self-phase matching,^{11,12} which led to high ($\sim 1.5\%$) tripling efficiency. The long interaction length was responsible for the high third-harmonic yield reported in Ref. 13. Stimulated Raman scattering has been investigated as well,¹⁴⁻¹⁷ and higher-order Stokes and anti-Stokes components have been observed on axis and on cones of different apex angles.

In this Letter we present experimental results on the properties of SBS pumped with a Bessel beam. The experimental setup is shown in Fig. 1. A frequency-doubled, Q-switched, injection-seeded Nd:YAG laser (Quanta Ray GCR-330) provides Fourier-transform-limited pulses of 6-ns duration at 532 nm. A Gaussian beam of 10-mm diameter passing through a

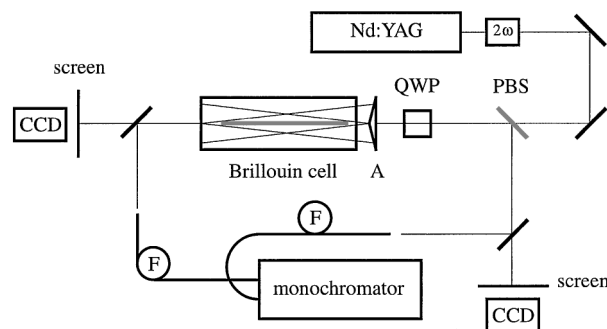


Fig. 1. Scheme of the experimental setup: PBS, polarization beam splitter; QWP, quarter-wave plate; A, 2.5° quartz axicon; CCD, CCD camera for beam-profile recording; F's, bare-tip single-mode fibers. A double fiber-input monochromator is used for frequency measurements.

quartz axicon (conical lens) with an apex angle of 175° is converted into a nearly Bessel–Gauss beam of $w = 5$ mm and $\gamma \approx 1.25^\circ$. The entire region of diffraction-free propagation is covered by a 30-cm Brillouin cell filled with distilled and filtered (200-nm particle-size) water. In our experiment water was preferentially used because of its moderate Brillouin gain, $g_B = 0.0048$ cm/MW, low phonon lifetime, $\tau \approx 300$ ps, relatively large Brillouin shift, $\Omega_B = 7.4$ GHz (Ref. 18), and low Raman gain. The backscattered beam is extracted by its polarization. The beam profiles of both the forward- and backward-scattered beams are recorded by a CCD camera. Light from localized regions within both the forward- and the backward-scattered beams is extracted by bare-tip single-mode fibers and transported into a grating monochromator equipped with a CCD camera at the exit for spectral analysis. Multimode fibers are used to send light to a fast photodiode (Hamamatsu G4176, 100 ps) read by a fast digitizing oscilloscope (Tektronix TD680B 1 GHz, 5 Gsamples) for pulse-duration measurements.

First, the phase-conjugation property of the Stokes signal was investigated. As shown in Fig. 2(a), the backscattered beam has a ring shape, unlike the Gaussian pump beam, the reflection of which is placed on the right-hand side of the SBS beam. No phase conjugation was observed just above the SBS threshold. This result can be explained in the following way: Owing to the noncollinear phase matching in the Brillouin cell, a backscattered signal is generated on axis, and hence a strong Gaussian-like backward-scattered Stokes beam is created and, after it passes through the axicon again, is transformed into a Bessel–Gauss beam, which in the far field has a ring shape [Fig. 2(a)] and divergence of ≈ 10 mrad. This value is somewhat less than the pump-beam divergence of ≈ 17 mrad [Fig. 2(c)], owing to the intrinsic initial divergence of the SBS beam emerging from the narrow line focus in the cell. After the pump-pulse energy is increased, the backward-propagating first Stokes reaches threshold for second-order Stokes generation in the forward direction—a highly directional Gaussian-like beam seen in the center of Fig. 2(d). The spectrum of the forward on-axis beam is shown in Fig. 3(a), in which a single line, shifted by $-2\Omega_B$ from the laser frequency ω_L , can be seen. A further increase of the input pulse energy leads to its reaching a third threshold when the second-order Stokes pulse owing to its extended propagation distance in the line focus can generate a third-order Stokes pulse in the backward direction. A spectrum of the backscattered beam is shown in Fig. 3(b), in which the presence of two frequencies, $\omega_L - \Omega_B$ and $\omega_L - 3\Omega_B$, is evident. To visualize better the position of the odd-order Stokes frequencies we focused the backscattered beam, containing the first- and third-order Stokes, into the single-mode fiber that was used as input for the monochromator. Owing to forward four-wave mixing in the fiber,² many equidistant frequencies, separated by $2\Omega_B$, are generated, forming the frequency ruler shown in Fig. 3(c).

When the pump-pulse energy is increased, the backscattered output beam changes its intensity distribution, which features an intense central maximum surrounded by a halo [Fig. 2(b)], again far from phase conjugation compared with the input beam. When the peak intensity is increased, not only the central lobe but also the adjacent secondary rings reach SBS threshold in the collinear phase-matching geometry, thus providing conditions for better phase conjugation. This effect was more clearly observed when the ring beam created by the axicon was sharply focused into the Brillouin cell. The line focus in that case was very short (equal to the Rayleigh range of the envelope Gaussian beam); thus none of the higher-order interactions described above could take place. The output SBS beam observed was phase conjugated to the input beam. In this study, however, we are interested in SBS with diffraction-free beams, whereas the latter case, although it leads to improved phase conjugation, is that of a Gauss-dominated Bessel–Gauss beam,

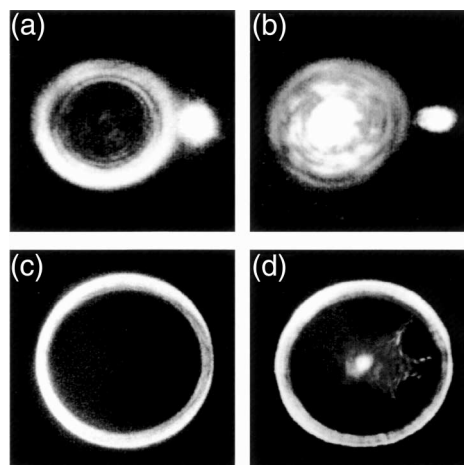


Fig. 2. Far-field images of the output beams: (a) backward SBS at low peak power above the threshold (no phase conjugation), (b) backward SBS at high energy in the pulse, (c) pump beam, (d) pump beam (ring) and a second SBS (central spot) after the second threshold.

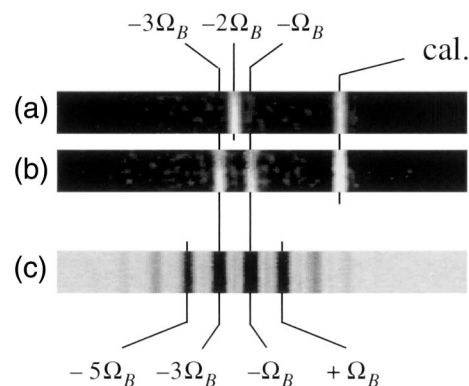


Fig. 3. Spectra recorded by the grating monochromator: (a) central spot in the forward direction, where the second Stokes frequency is visible, (b) backward-scattered beam with third and first Stokes frequencies, (c) four-wave mixing inside the fiber used as a ruler for the relative frequency measurements. The line labeled cal. is a reference frequency.

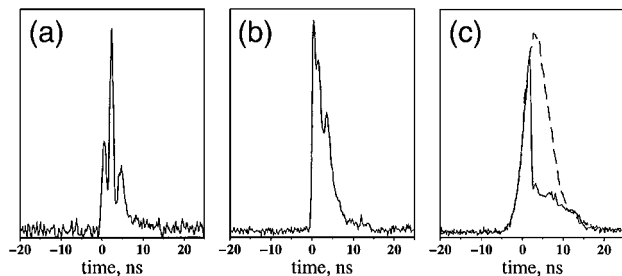


Fig. 4. Typical temporal pulse shapes: (a) backward-scattered pulse, (b) forward-scattered second Stokes, (c) pulse shape in the forward ring. In (c) the outer part of the ring (solid curve) is affected by the stimulated scattering, whereas the inner part (dashed curve) is not affected by the interaction.

which is similar to most experimental realizations of phase conjugation with phase-distorted Gaussian beams.

Temporal profile measurements of typical pulses recorded in backward [Fig. 4(a)] and forward [Figs. 4(b) and 4(c)] direction reveal similarities with SBS in optical fibers. In Figs. 4(a) and Fig. 4(b) regular subpulses can clearly be seen, separated by ≈ 1.3 ns, which is exactly the line-focus length L in the Brillouin cell. The formation of the substructure can be considered an onset of Brillouin mode locking, analogous to the same effect observed in optical fibers.³ The advantage of using a Bessel beam in a bulk medium is, however, that high-energy pulses can be studied without self-phase modulation or optical damage in a gain-guided geometry.¹⁶ In Fig. 4(c) the pulse shapes recorded in the inner (dashed curve) and the outer (solid curve) parts of the forward ring are shown. The inner part of the ring, which is an image of the wings of the Gaussian pump beam, does not reach SBS threshold (owing to its low intensity), and therefore the pulse shape reproduces the pump pulse exactly. The outer part of the ring is an image of the central part of the pump beam and is therefore affected by the interaction—the sharp cutoff that was observed reflects the onset of the SBS process. In contrast to SBS with Gaussian beams, in which practically all the pump energy is transferred into the backward Stokes beam, in our case, owing to the second-order Stokes generation, the forward output efficiency remains high.

In conclusion, we have investigated the spatial, spectral, and temporal properties of the process

of stimulated Brillouin scattering pumped by a Bessel–Gauss beam. The poor phase-conjugation fidelity of the backscattered signal is attributed to the noncollinear nature of the scattering process, involving a conical beam. The extended (≈ 30 -cm) interaction region, along the diffraction-free propagation of the pump beam, offers a unique possibility to observe higher-order SBS, which in the case of a focused Gaussian beam cannot be done in pure form. Stokes orders as high as the third were recorded.

The authors are grateful to V. Tugbaev (Institute of Physics, Minsk, Russia) for providing the axicon through INTAS-Belarus 97-0533 and to the Netherlands Foundation for Fundamental Research on Matter (FOM) for financial support. I. Velchev's e-mail address is iavor@nat.vu.nl.

References

1. K. O. Hill, D. C. Johnson, and B. S. Kawasaki, *Appl. Phys. Lett.* **29**, 185 (1976).
2. P. Labudde, P. Anliker, and H. P. Weber, *Opt. Commun.* **32**, 385 (1980).
3. B. S. Kawasaki, D. C. Johnson, Y. Fujii, and K. O. Hill, *Appl. Phys. Lett.* **32**, 429 (1978).
4. D. T. Hon, *Opt. Lett.* **5**, 516 (1980).
5. C. Brent Dane, W. A. Newman, and L. A. Hackel, *IEEE J. Quantum Electron.* **30**, 1907 (1994).
6. I. Velchev, D. Neshev, W. Hogervorst, and W. Ubachs, *IEEE J. Quantum Electron.* **35**, 1812 (1999).
7. J. Durnin, J. J. Miceli, Jr., and J. H. Eberly, *Phys. Rev. Lett.* **58**, 1499 (1987).
8. J. Durnin, *J. Opt. Soc. Am. A* **4**, 651 (1987).
9. J. Durnin, J. J. Miceli, Jr., and J. H. Eberly, *Opt. Lett.* **13**, 79 (1988).
10. F. Gori, G. Guattari, and C. Padovani, *Opt. Commun.* **64**, 491 (1987).
11. B. Glushko, B. Kryzhanovsky, and D. Sarkisyan, *Phys. Rev. Lett.* **71**, 243 (1993).
12. S. P. Tewari, H. Huang, and R. W. Boyd, *Phys. Rev. A* **51**, R2707 (1995).
13. C. Altucci, R. Bruzzese, D. D'Antuoni, C. de Lisio, and S. Solimeno, *J. Opt. Soc. Am. B* **17**, 34 (2000).
14. S. Klewitz, P. Leiderer, S. Herminghaus, and S. Sogomonian, *Opt. Lett.* **21**, 248 (1996).
15. L. Niggl and M. Maier, *Opt. Lett.* **22**, 910 (1997).
16. L. Niggl and M. Maier, *Opt. Commun.* **154**, 65 (1998).
17. V. Vaičaitis, A. Stabinis, A. Marcinkevičius, and V. Jaritis, *Opt. Commun.* **178**, 461 (2000).
18. R. W. Boyd, *Nonlinear Optics* (Academic, San Diego, Calif., 1992).